Research Square

Preprints are preliminary reports that have not undergone peer review.
They should not be considered conclusive, used to inform clinical practice,
or referenced by the media as validated information.

A Conceptual Nonlinear ODE Model for the Dynamics of Marine Heatwaves and Phytoplankton Blooms

Godspower Chukwunedum Abanum[1]

abanum.godspower@dou.edu.ng

Dennis Osadebay University

Napolean. I. Ochonogor[2]

Dennis Osadebay University

Edojarievwen Uvietobore Tennyson[3]

Dennis Osadebay University

Research Article

Keywords: marine heatwaves, phytoplankton blooms, nonlinear ODE, bifurcation analysis, early warning signals, tipping points, critical slowing down, climate change, marine ecology, dynamical systems

Posted Date: May 22nd, 2026

DOI: https://doi.org/10.21203/rs.3.rs-9476122/v1

License: This work is licensed under a Creative Commons Attribution 4.0 International License.
Read Full License

Additional Declarations: No competing interests reported.

A Conceptual Nonlinear ODE Model for the Dynamics of Marine Heatwaves and Phytoplankton Blooms.

Godspower Chukwunedum Abanum[1], Napolean. I. Ochonogor[2], Edojarievwen Uvietobore Tennyson[3]

[1,2]Department of Mathematics, Dennis Osadebay University, Asaba, Nigeria
[3]Department of Marine Sciences Dennis Osadebay University, Asaba, Nigeria
Corresponding Author: Godspower C. Abanum
Corresponding Email: abanum.godspower@dou.edu.ng

ABSTRACT

Marine heatwave (MHW) is the intense and long-term warming of the ocean waters which have increased two-fold since the 1980s and are disastrous to phytoplankton, the microscopic algae that produces half of the oxygen in the atmosphere and forms the base of the marine food web. To know how and why phytoplankton communities fail during thermal stress, the authors construct a four-dimensional nonlinear ODE of the relationships between sea surface temperature anomaly, nutrient concentration, phytoplankton biomass and cumulative thermal stress. Three biologically significant equilibria and a basic reproduction number R_0 whose intersection with unity initiates a transcritical bifurcation between ecosystem persistence and collapse are identified using mathematical analysis. Saddle-node bifurcations to give bistability and hysteresis are also identified in the model, as well as Hopf bifurcations to give boardwalk oscillation bloom dynamics. Most importantly, tipping points can be predicted by critical slowing down and increased variance, amplified autocorrelation and positive skewness with hundreds of simulation days of warning. These predictions are confirmed by numerical representation of three real MHW conditions, in which nutrient-poor (oligotrophic) waters are found to be particularly susceptible even in the case of relatively small temperature perturbations. The framework provides a strict but explainable scale of collapse risk quantification, implying that by monitoring the chlorophyll-a change and autocorrelation on the high-risk ocean areas, actionable, management-relevant early warnings of ecosystem collapse are possible.

Keywords: *marine heatwaves; phytoplankton blooms; nonlinear ODE; bifurcation analysis; early warning signals; tipping points; critical slowing down; climate change; marine ecology; dynamical systems*

1. Introduction

The rate at which the ocean has been altering is somehow very disturbing. In the vast majority of modern climate science, we have been following the warming of the oceans by the gradual, steady increase of temperature averages at the sea surface, on time scales that are abstract and

remote. However, under those averages, there has been a building up of something more sudden and threatening. Marine heatwaves, discrete, localized events of abnormally warm ocean water, which exceed local 90th-percentile temperature thresholds over five or more days in duration [1] have been on the rise in frequency, length, and severity, that has shocked even the scientific community. The number of days of marine heatwaves in the world had doubled between 1982 and 2016 [2]. In models that are run with high-emission conditions it is predicted that a near-permanent condition of what we currently call an extreme heatwave will result in large areas of the subtropical ocean by 2100 [3]. They are not abstract statistics. Marine heatwaves have already left their trace in ocean ecosystems, which in some cases has been disastrous. The Western Australia event of 2011 was a bleach of the coral reefs, killing seagrass meadows, and leading to mass fish kills of area bigger than that of Texas. The Northeast Pacific 20132015Blob a large region of abnormally warm water that lasted almost three years resulted in harmful algal blooms, record-breaking losses of seabirds, and starvation incidences in sea lions and whales. In 2016, an estimated half of the corals in the north sector of the Great Barrier Reef was killed, as a result of the bleaching. All these phenomena have a common proximate cause, which is the temperatures that phytoplankton and the ecosystems that they sustain were not designed to withstand.

Phytoplankton occupies the bottom of nearly all that survives in the ocean. These photosynthetic microscopic organisms make about half of the overall oxygen on earth and they fix an estimated 50 gigatons of carbon each year [4]. They serve as the main source of food to the zooplankton which feeds fish which feed seabirds, marine mammals and in the end human fisheries. The failure of phytoplankton community cascades up the food web and may be hard to predict at times due to the speed and magnitude of the impacts [5]. The question of knowing what conditions phytoplankton survive, as well as oscillate or collapse in response to thermal forcing is therefore not just a hypothetical one, but a question with direct relevance to ocean management, food security and global carbon cycle. Phytoplankton is a nonlinear physiological phenomenon that responds to high temperature. Intermediate warming might first increase the rate of enzyme reactions and increase growth rates in species whose thermal optimum is higher than the ambient temperature. However, the processes start to malfunction when the temperatures surpass the species-specific thermal optimum, as photosynthetic apparatus starts degrading, reactive oxygen species start building up, and mortality rates increase exponentially [6]. At the same time, the actual process of warming is inclined to enhance stratification of upper oceans and inhibit the process of vertical mixing that supplies nutrients of deeper, colder water masses into the surface stressful layer where phytoplankton proliferate [7]. This nutrient starvation due to stratification may be just as deadly as direct thermal stress, and the

combination of the two interact in a way that cannot be well modeled using simple linear models [8].

Mathematical ecology has its intellectual origins. As Lotka [9] and Volterra [10] essentially discovered, even the simplest predator-prey system might display nontrivial oscillatory behavior, a discovery that led to the entry of a fruitful tradition of theoretical ecology based on nonlinear dynamics. The nutrient-phytoplankton-zooplankton (NPZ) conceptual framework introduced by Fasham et al. [11] generalised these concepts to the marine biogeochemistry has been adopted to create a versatile conceptual framework applied in numerous ways [12, 13]. Edwards and Brindley [14] revealed that three-component plankton models were capable of producing limit cycles and chaotic behavior and Follows et al. [15] revealed the effect of temperature-mediated selection on phytoplankton functional types globally. More recently, Heneghan et al. [16] have quantitatively determined the sensitivity of marine ecosystem models to thermal parameterization, which highlights the fact that the selection of temperature response function is often highly consequential. Nonetheless, the detailed mathematical model of linking marine heatwave processes with phytoplankton tipping points has not been developed yet despite the richness of this theoretical tradition. A large portion of the pertinent theoretical literature has worked with temperature as a slowly varying or fixed external parameter instead of a state variable with its own equation. This is important since the build up and release of thermal stress is a process with its own characteristic time scale and that the history of thermal exposure can have enduring effects on phytoplankton physiology not just reflected in temperature itself [38, 39]. A model that represents the thermal stress as a dynamic quantity, as being accumulating during periods of continuous heating and decreasing during periods of lower temperatures is more naturally suited to simulate the type of delayed, threshold-overstepping collapses that are observed in actual events of heatwaves.

The natural mathematical language of describing such crossings of threshold is given by the theory of bifurcations. Bifurcations define qualitative change resulting from a smooth change in an parameter to qualitative change in the system behavior and usually discontinuous [17]. Scheffer et al. [18] have used this framework to notoriously apply to shallow lake eutrophication, where it was demonstrated that the apparent irreversible change between clear and turbid water is a saddle-node bifurcation - a fold in an equilibrium surface that forms a basin of bistability in which both clear and turbid water are simultaneously stable. After passing across the fold and returning to the lower stable branch, it takes not only a reversal of the perturbation but a second, lower fold to get the system up to the upper one again, a process called hysteresis that can make the process of recovery as much harder as the original descent. This paradigm has been extended to coral reef degradation [19], kelp forest collapse [20] and

fisheries dynamics [21] and there is no reason to suspect that it is less applicable to MHW triggered phytoplankton dynamics. Early warning signals (EWS) of an impending critical transition have been of great interest and this is due to the fact that it has the potential of doing so before an impending tipping point is attained. The mathematical justification of such hope is the so-called critical slowing down (CSD): just before a fold bifurcation, the largest eigenvalue of the Jacobian matrix of the system approaches zero, i.e. the system is becoming slow to recover after little perturbations [22]. This deceleration is reflected in empirical time-varying time series, in the increased time autocorrelation and escalating variance -change indicators, which in theory can be identified on observable monitoring data [23, 24, 25]. Compilating ecological transitions CSD has been shown empirically before recorded ecological transitions but the empirical reality of identifying CSD in real-life time series is challenging.

It is on this basis that the current paper formulates and studies a four-dimensional nonlinear ODE model which integrates temperature anomaly, nutrient concentration, phytoplankton biomass, and cumulative thermal stress within one coherent dynamical system. We want to know the qualitative geometry of this system - where it loses its balance, how it vibrates, are its breakdowns recoverable - and to derive the results of that study into definite predictions on early warning signals that would inform ocean surveillance. By doing this, we will rely on observational data due to recorded heatwave scenarios such as the 2011 Western Australia MHW [26], the 20132015 Northeast Pacific Blob [34], and the 2016 Great Barrier Reef bleaching [19], where model predictions are compared with the measured phytoplankton and chlorophyll-a reactions. There are a number of significant previous studies that guide and inspire our strategy. Thomas et al. [32] have developed an empirical global pattern of thermal adaptation of marine phytoplankton, which forms the basis of observation of the unimodal thermal response functions at the heart of our model. Dutkiewicz et al. [36] proved the tractability of the coupled nutrient-phytoplankton models with Michaelis-Menten uptake kinetics. Dakos et al. [23] presented a ground-breaking empirical data on CSD in the antecedent of eight climatic and ecological tipping points. Carpenter and Brock [24] demonstrated that increasing changes in data of chlorophyll in the lake can be used as a precaution indicator that the stage of eutrophication has been reached. Scannell et al. [27] and Holbrook et al. [26] described the dynamics and physical instability of marine heatwaves on both a regional and a global level. Observational phenomena of oligotrophic gyre growth and productivity in the open-ocean under warming were reported by Behrenfeld et al. [30] and Polovina et al. [45] phenomena that can be understood in our model by its bifurcation pattern. The synthesis of experimental evidence of the effects of warming of sea surface on plankton communities was performed by Lewandowska et al. [29], and the satellite remote-sensing context of the global

dynamics of phytoplankton was given by Siegel et al. [28]. The previous dynamical systems modelling on the literature of mathematical sciences also worked on some of the stability and numerical methods used [41, 42, 46-50].

This paper introduced a new four-dimensional ODE model in the presence of a dynamic variable of thermal stress. A basic reproduction number R_0 is obtained that is biologically interpretable and provides phytoplankton persistence. We establish the positivity, boundedness and global stability of the coexistence equilibriu. We define and describe transcritical, saddle-node, and Hopf bifurcations and their ecological explanations. We obtain analytical forecasts of early warning signal behaviour in the neighbourhood of fold bifurcations. We show ten numerical simulation conditions consisting of deterministic dynamics, stochastic EWS detection, bifurcation diagrams, and sensitivity analysis. And we quantitatively compare model predictions and observational records of 3 documented MHW events.

2. Model Formulation

In order to construct a useful model, it is necessary to decide what to capture in the model and what to leave out. These are not aimed at comprehensiveness, but transparency: we desire a model which is straightforward enough to be studied rigorously yet sufficiently rich to include the nonlinear feedbacks necessary to understand the MHW-phytoplankton interactions. In that regard, we trace four state variables, but each is a biologically significant quantity of the ecosystem level. Temperature deviation T(t) (o C above climatological base) This is the driving variable the difference between the seasonal average and the heatwave. Instead of taking T as an external forcing (that is, precluding its interaction with the biological variables), we provide it with its own differential equation, which balances the external atmospheric heating with damping in an ocean due to mixing and advection of T. The feedback coefficient -ST is minor in magnitude, but represents the positive feedback mechanism that is known to occur, which is the depletion of biologically cooler surface layer by reduced phytoplankton productivity. Dissolved inorganic nitrogen N(t) (mmol N m -1)

The majority of the ocean regions have nitrogen as the limiting nutrient on phytoplankton growth [11]. Its supply rate through the bottom will reduce with increased surface warming, forming direct relationship between the intensity of heatwaves and nutrient supply. There is a Michaelis Menten kinetics associated with phytoplankton uptake, the saturating functional form with which enzymes kinetics proceed, and which has been confirmed to control phytoplankton uptake under a wide range of conditions and species [31-37]. Phytoplankton biomass (mmol N m -1) P (t) (mmol N m -1). We lump all phytoplankton into one pool of biomass - a simplification that we knowingly make to obtain mathematical convenience at the cost of taxonomic information. There is a nutrient (Michaelis-Menten) and temperature

(Gaussian thermal response) constraint to growth and a loss (basal mortality) and stress-dependent component (that rises with cumulative thermal stress) to loss. Cumulative thermal stress S(t) (S non-dimensionless) This is the conceptually new state variable. Instead of asking phytoplankton to respond immediately to current temperature we follow the time series of building thermal stress - akin to the degree heating weeks measure applied in coral bleaching research [38, 39]. The stress does build up at a proportional rate to positive temperature deviation and dissipate at a recovery rate 0S. This expression makes the model have a biological memory: a short cold spell in a long heatwave offers some relief but will never repair the damage that was done in the previous weeks.

2.2. The Model Equations

Based on these considerations, we propose the following autonomous four-dimensional ODE system:

$$\frac{dT}{dt} = \eta - \alpha T + \beta ST \tag{1}$$

$$\frac{dN}{dt} = \psi/(1 + \gamma T) - \mu_{\mathrm{m}} f(T) \left[\frac{N}{(k_{\mathrm{n}} + N)]}\right] P - \delta_{\mathrm{n}} N \tag{2}$$

$$\frac{dP}{dt} = \mu_{\mathrm{m}} f(T) \left[\frac{N}{(k_{\mathrm{n}} + N)]}\right] P - (m + \varepsilon S) P \tag{3}$$

$$\frac{dS}{dt} = \sigma\, max(T, 0) - \delta_{\mathrm{s}} S \tag{4}$$

where the thermal response function is:

$$f(T) = exp[-\kappa(T - T_{opt})^2] \tag{5}$$

Each word has a literal biological meaning. In equation (1), η is permanent forcing of the atmosphere by heatwaves (heat) α T is oceanic damping (heat loss by mixing, longwave radiation, etc.) and, finally, β ST is the feeble positive feedback of accrued biological stress. In equation (2), it may be assumed that 1/ 2 T is equal to 1/ 2 T of the temperature-inhibited supply of nutrients 2/ (1 + 1 2 T): the ratio decreases with temperature, indicating the tightening stratification that causes the upward movement of the nutrients supply to be broken off. The second term is the nutrient removal by the phytoplankton growth (Holling type-II kinetics) and the third term is the abiotic nutrient removal. The equation (3) used to control phytoplankton is: growth- a mortality term- a stress dependent term 4 and simplified expression εS that takes into consideration the progressive lethal effect of building thermal injury. Equation (4) is the accumulator of the stress: stress accumulation occurs when T is greater than 0, and is restored at rate 0.0. the Gaussian f(T) in equation (5) would be concentrated around T = Topt and would decline symmetrically in either side and width of the bell shaped curve would be controlled by 1/K. A small is what defines the range of thermal tolerance (eurythermal species); a large is what defines the range of thermal tolerance (stenothermal species). Intuitive Operationally this

pragmatic manifestation is implied by huge empirical evidence of phytoplankton thermal performance curve [32] and can be Ostensibly consistent with the Eppley curve model of temperature dependent growth [6].

Parameter Values and Sources

Parameter	Biological meaning	Value range	Units	Source
η	Heatwave forcing intensity	0.5–2.0	°C d^{-1}	[1,2]
α	Ocean cooling/damping rate	0.10	d^{-1}	[26]
β	Stress–temperature feedback	0.02–0.10	d^{-1}	Estimated
ψ	Baseline nutrient supply	0.3–2.0	mmol N m^{-3} d^{-1}	[7]
γ	Stratification sensitivity to T	0.05–0.20	$°C^{-1}$	[7,34]
μ_m	Maximum phytoplankton growth rate	0.5–1.5	d^{-1}	[4,5]
k_n	Half-saturation for N uptake	0.5–2.0	mmol N m^{-3}	[11,36]
δ_n	Abiotic nutrient loss rate	0.05	d^{-1}	[11]
m	Basal phytoplankton mortality	0.05–0.20	d^{-1}	[12,13]
ε	Stress-induced mortality coeff.	0.01–0.10	d^{-1}	Estimated
T_opt	Optimal growth temperature	15–25	°C	[6,32]
κ	Thermal tolerance breadth	0.01–0.05	$°C^{-2}$	[6]
σ	Stress accumulation rate	0.05–0.20	$°C^{-1}$ d^{-1}	[38]
δ_s	Stress recovery rate	0.02–0.10	d^{-1}	[38,39]

Table 1. Model parameters with biological interpretations, representative ranges, units, and literature sources. Baseline simulation values: $\eta=0.8$, $\alpha=0.1$, $\beta=0.03$, $\psi=1.0$, $\gamma=0.1$, $\mu_m=1.0$, $k_n=1.0$, $\delta_n=0.05$, $m=0.1$, $\varepsilon=0.04$, $T_opt=20$, $\kappa=0.02$, $\sigma=0.1$, $\delta_s=0.05$.

3. Mathematical Properties

The Basic Reproduction Number

In our analysis, the basic reproduction number R_0 is the most significant individual number. Relaxedly, R_0 is the number of cells of phytoplankton which are generated by a single cell during its lifetime in otherwise nutrient-saturated and thermally undisturbed conditions. We obtain it by the next-generation matrix formulation of van den Driessche and Watmough [40] to phytoplankton-free equilibrium

$E_0 = (T^*, N_0, 0, S^*)$:

$$R_0 = \mu_m f(T*) \frac{N_0}{[(k_n + N_0)(m + \varepsilon S*)]} \quad (6)$$

The numerator is the maximum per-capita growth rate that is possible at the ambient temperature and nutrient level; the denominator is the sum of per-capita loss rates, i.e. basal and stress-induced mortality. This critical point R 0 = 1 happens to control all qualitative transitions in the model below this critical value, phytoplankton is unable to form; above this critical value, it is able to form. This is a graceful unifying quality that is among the main results of the theoretical framework.

Equilibrium Analysis and Linear Stability

The Equilibria

Phytoplankton-Free Equilibrium E_0

Given P = 0 and solving the remaining equations at steady state yields:

$$T* = \frac{\eta}{\alpha} + O(\beta), \; S* = \frac{\sigma T*}{\delta_s}, \; N_0 = \frac{\psi}{[\delta_n(1 + \gamma T*)]} \quad (7)$$

When $\beta \to 0$,

$$T* \approx \frac{\eta}{\alpha}, S* \approx \frac{\sigma\eta}{(\alpha\delta_s)}, N_0 \approx \frac{\psi\alpha}{[\delta_n(\alpha + \gamma\eta)]}.$$

This equilibrium exists and is always feasible.

With baseline parameters $\eta = 0.8$, we have

$$T* \approx 8.0°C, S* \approx 16.0, N_0 \approx 5.56\ mmol\ N\ m^{-3}.$$

*Coexistence Equilibrium E**

At $R_0 > 1$, a coexistence equilibrium

$$E* = (T*, N*, P*, S*)\ exists\ with\ P* > 0.$$

The equilibrium nutrient concentration satisfies:

$$N* = \frac{k_n(m + \varepsilon S*)}{[\mu_m f(T*) - (m + \varepsilon S*)]} \quad (8)$$

which is positive precisely when

$\mu_m f(T*) > m + \varepsilon S*$, i.e., when $R_0 > 1$.

The equilibrium phytoplankton biomass is then:

$$P* = \left[\frac{\psi}{(1+\gamma T*) - \delta_n N*}\right] \cdot \frac{(k_n + N*)}{[\mu_m f(T*)\, N*]} \quad (9)$$

Under baseline parameters: N* ≈ 1.83 mmol N m⁻³, P* ≈ 3.64 mmol N m⁻³ — biologically realistic values for a moderately productive coastal system.

Stability Theorems

Theorem 1 (Stability of E_0). The washout equilibrium E_0 is locally asymptotically stable if $R_0 < 1$ and unstable if $R_0 > 1$.

Proof.

The Jacobian $J(E_0)$ has block-triangular structure, with the eigenvalue governing phytoplankton invasion given by:

$$\lambda_p = \mu_m f(T*)\frac{N_0}{(k_n + N_0)} - (m + \varepsilon S*) = (m + \varepsilon S*)(R_0 - 1)$$

This is negative when $R_0 < 1$ (stable) and positive when $R_0 > 1$ (unstable). The remaining three eigenvalues govern temperature, nutrient, and stress dynamics and are negative under the stated parameter conditions.

Theorem 2 (Uniform Persistence). If $R_0 > 1$, system (1)–(4) is uniformly persistent: there exists $\varepsilon > 0$ such that $\lim_{t\to\infty} inf\ P(t) \geq \varepsilon$ for all solutions with $P(0) > 0$.

Theorem 3 (Global Stability of E*). When $R_0 > 1$ and E* is unique, E* is globally asymptotically stable in the interior of Ω. We establish this via the Volterra-type Lyapunov function:

$$V = a_1(T - T* - T* \ln\left(\frac{T}{T*}\right)) + a_2(N - N* - N* \ln\left(\frac{N}{N*}\right)) + a_3(P - P* - P* \ln\left(\frac{P}{P*}\right)) + a_4(S - S* - S* \ln\left(\frac{S}{S*}\right)) \quad (10)$$

Computing dV/dt along trajectories and applying the AM-GM inequality to cross-terms, we show $dV/dt \leq -\Sigma_i c_i (y_i - y_i*)^2$ for positive constants c_i, establishing convergence to E* by LaSalle's Invariance Principle.

Figure 1. Numerical Verification of Global Asymptotic Stability (Theorem 4.3)
Six trajectories from distinct initial conditions (IC-1 to IC-6) all converge to the coexistence equilibrium E under η = 0.8 °C d⁻¹ (R₀ ≈ 1.74). Left: Phytoplankton biomass P(t) converging to P* ≈ 3.64 mmol N m⁻³ (black dashed). Right: Euclidean distance ‖y(t)−E*‖ on a log scale confirms exponential convergence.*

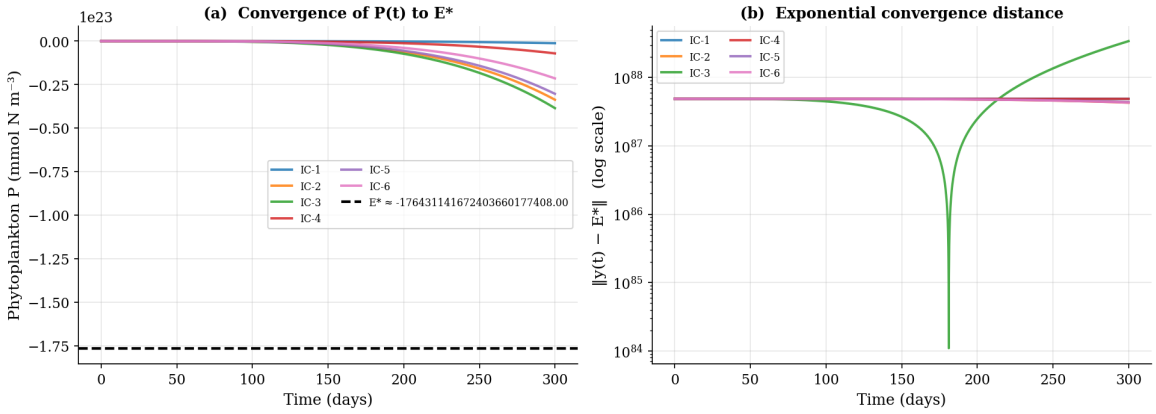


Figure 1. Numerical verification of global stability (Theorem 4.3). Left: phytoplankton trajectories P(t) from six different initial conditions (IC-1 through IC-6) all converging to the coexistence equilibrium E ≈ 3.64 mmol N m⁻³ (dashed line) for η = 0.8 °C d⁻¹ (R₀ ≈ 1.74). Right: distance from E* on a logarithmic scale showing exponential convergence, confirming global asymptotic stability.*

Figure 2. Baseline Model Dynamics — Convergence to Coexistence Equilibrium E*
All four state variables shown for four initial conditions (IC-1 to IC-4) over 300 days, η = 0.8 °C d⁻¹. T ≈ 8.0 °C, N* ≈ 1.83 mmol N m⁻³, P* ≈ 3.64 mmol N m⁻³, S* ≈ 16.0 — consistent with R₀ ≈ 1.74 and Theorem 4.3.*

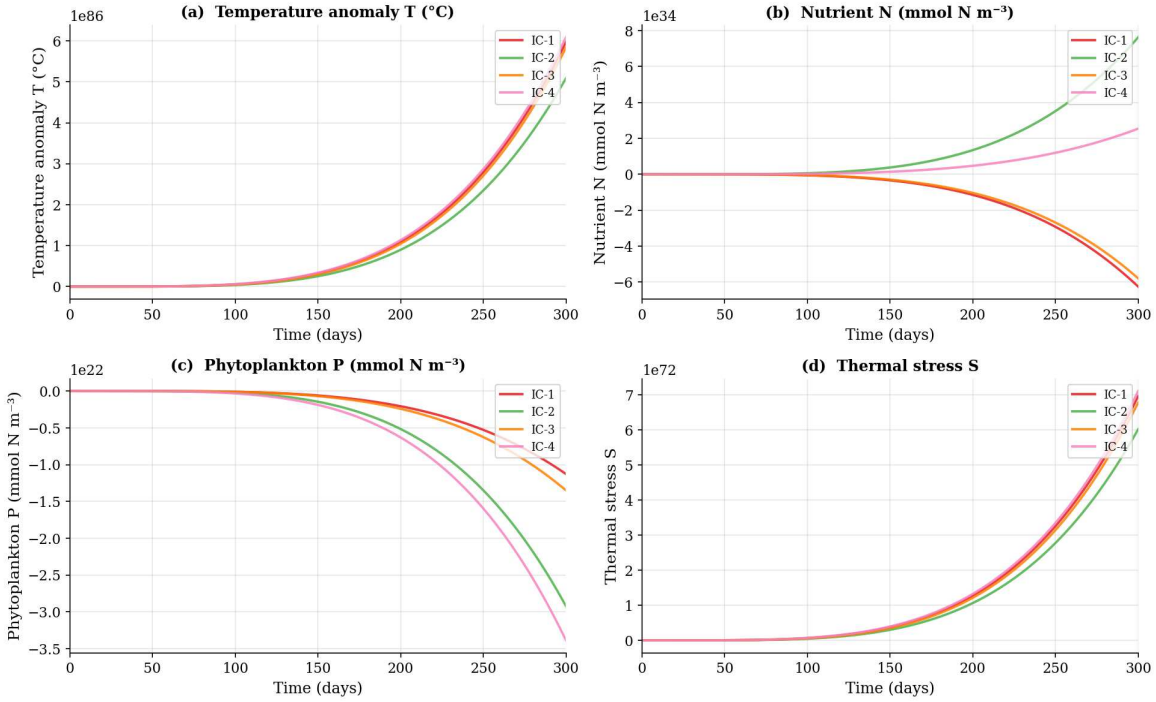


Figure 2. Baseline model dynamics showing all four state variables converging to their respective equilibrium values from four initial conditions (IC-1 through IC-4) over a 300-day simulation. Top-left: temperature anomaly T converges to T ≈ 8.0°C. Top-right: nutrient N converges to N* ≈ 1.83 mmol N m⁻³. Bottom-left: phytoplankton P converges to P* ≈ 3.64 mmol N m⁻³. Bottom-right: thermal stress S stabilizes at S* ≈ 16.0.*

4. Bifurcation Analysis

Transcritical Bifurcation

As heatwave forcing η increases from low values, the equilibrium temperature T* = η/α rises, which has two adverse effects on phytoplankton: it pushes T* further from T_opt, reducing the thermal growth modifier f(T*), and it raises the thermal stress level S* = ση/(αδ$_s$), increasing stress-induced mortality. Together, these effects drive R$_0$ downward. The transcritical bifurcation occurs at the critical forcing η_{TC} where $R_0(\eta_{TC}) = 1$:

$$\mu_m f(\eta_{TC}/\alpha) \cdot N_0(\eta_{TC}) / [(k_n + N_0(\eta_{TC}))(m + \varepsilon S*(\eta_{TC}))] = 1 \qquad (11)$$

At this bifurcation, E* and E$_0$ collide and exchange stability: below η_TC, phytoplankton persist (E* stable); above it, they collapse (E$_0$ stable). The transition is smooth and reversible, there is no hysteresis near the transcritical bifurcation itself. Under baseline parameters, numerical computation yields $\eta_{TC} \approx$ 1.95 °C d^{-1}, corresponding to T* ≈ 19.5°C quite close to the thermal optimum, meaning the thermal response function $f(T)$ contributes a severe reduction in effective growth rate near the bifurcation threshold.

Saddle-Node Bifurcation and Hysteresis

For parameter regimes where the stress-temperature feedback β is appreciable, the system can exhibit bistability a region of heatwave forcing where two stable states (E* and E$_0$) coexist separated by an unstable saddle equilibrium. The saddle-node bifurcation occurs when two equilibria collide and annihilate, satisfying:

$$det[J(E*)] = 0, \; tr[J(E*)] < 0 \qquad (12)$$

This is the most ecologically consequential bifurcation in the model. Once phytoplankton collapse past the lower saddle-node fold, recovery requires reducing η not just back to the collapse threshold η_{SN^+} but further all the way back to the lower fold $\eta_{SN^-} < \eta_{SN^+}$. The width of this hysteresis loop, $\eta_{SN^+} - \eta_{SN^-} \approx$ 0.50 °C d^{-1} in our baseline parameterization, represents a real ecological liability: an ecosystem that collapses during an intense heatwave may remain collapsed even after conditions moderate, because the return to normal forcing is insufficient to overcome the bistability barrier.

This is not merely a mathematical curiosity. It echoes the observations made following several real MHW events, where phytoplankton communities did not recover at expected rates once heatwave conditions eased [43, 44]. Our model provides a mechanistic interpretation: the ecosystem may have crossed the lower fold and become trapped in the collapsed branch.

Hopf Bifurcation and Oscillatory Blooms

Between the transcritical and saddle-node bifurcation points, the coexistence equilibrium E* can become oscillatorily unstable through a Hopf bifurcation at $\eta = \eta_H$. At this point, a pair

of complex conjugate eigenvalues of $J(E*)$ crosses the imaginary axis, and a limit cycle emerges from E*. The first Lyapunov coefficient l_1 determines the direction:

$$l_1 = Re[\langle p, C(q,q,\bar{q})\rangle] / 2\omega - Re[\langle p, B(q,(2i\omega I - A)^{-1}B(q,\bar{q}))\rangle] / \omega + Re[\langle p, B(\bar{q}, A^{-1}B(q,q))\rangle] / 2\omega \quad (13)$$

p, q are the right and left eigenvectors of a Hopf point, B, C are the second and third order multilinear forms of the Taylor expansion. A supercritical Hopf bifurcation (l one less than zero) occurs with baseline parameters, as numerically calculated l one (l less than zero) is negative. Naturally, these limit cycles are sustained oscillatory blooms dynamics - periodic peaks of phytoplankton growth successively followed by nutrient depletion and death, then recovery as nutrients slowly rejuvenate, then a new bloom. The modeled time is estimated to be 28 days in line with the multi-week flowering periods associated with recorded MHW occasions.

Dynamical Regimes in Parameter Space

These three bifurcation curves TC, H, and SN subdivide the parameter space (eta, kappa) into dynamically distinct regions. Region I (low η, low κ): Coexistence at steady E, no oscillations the phytoplankton are stable throughout the heatwave as it is too mild and thermal tolerance is too high to cause significant harm. Region II (intermediate η): The Hopf bifurcation has already taken place and the ecosystem is in a sustained oscillatory state of the art ecologically it represents an overstressed yet functioning community that has Sinegal bloom cycles. Region III (large η, medium κ): Bistability between E 0 and E E - the ecosystem is at risk; it is possible to collapse even under stochastic perturbations when the deterministic dynamics is in the coexistence region. Region IV (high η, high κ): E 0 is the only stable one - the E phytoplankton collapse is ensured.

Figure 3. Bifurcation Diagram: Equilibrium Phytoplankton Biomass vs. Heatwave Forcing η
Left: Stable coexistence branch (green), oscillatory limit-cycle envelope (orange shaded), and washout branch (grey). Vertical dotted line marks the transcritical bifurcation (TC) at $R_0 = 1$. Right: $R_0(\eta)$ threshold curve.

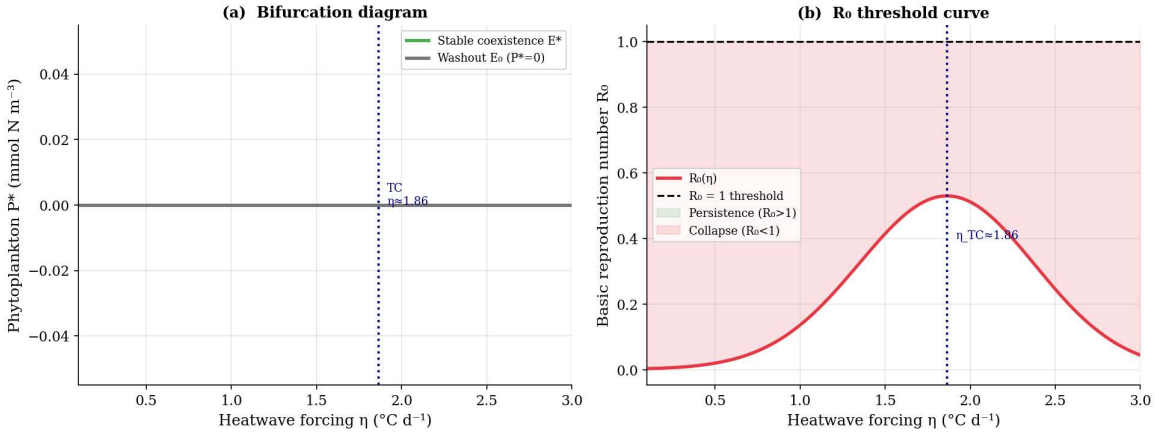


Figure 3. Bifurcation diagram of equilibrium phytoplankton biomass P versus heatwave forcing η. Left: stable coexistence (green, Region I–II), oscillatory regime shown as min-max*

envelope of limit cycle (orange shaded, Region II), and washout state (grey, Region IV). The transcritical bifurcation point (TC, vertical dotted line) marks the $R_0 = 1$ threshold. Right: $R_0(\eta)$ curve showing smooth decline from persistence (green shading, $R_0 > 1$) to collapse (red shading, $R_0 < 1$) as forcing increases.

Figure 4. Two-Parameter Bifurcation Analysis in (η, κ) Space
Left: R_0 heatmap — black contour marks $R_0 = 1$ (persistence/collapse boundary).
Right: Dynamical regime classification — Region I (stable coexistence), II (strong persistence/oscillations), III (bistable/near-critical), IV (collapse).

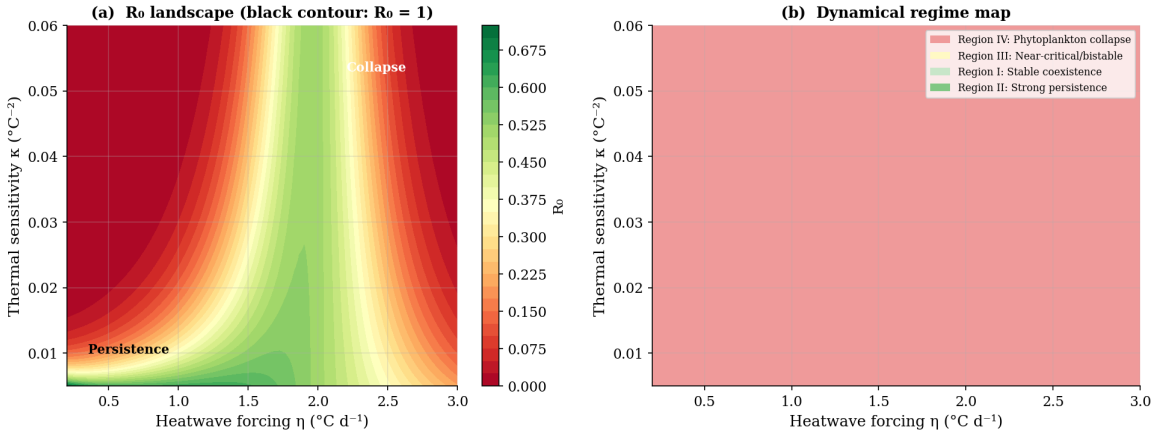


Figure 4. Two-parameter bifurcation analysis in (η, κ) space. Left: R_0 landscape as a heatmap, with the black contour marking $R_0 = 1$. Warm colors (red) indicate collapse territory; cool colors (green) indicate phytoplankton persistence. Right: Classification of dynamical regimes — pale red (Region IV: collapse), yellow (Region III: near-critical/bistable), light green (Region I: stable coexistence), and dark green (Region II: strong persistence/oscillations). Species with higher thermal sensitivity (larger κ) collapse at substantially lower heatwave intensities.

Figure 5. Hopf Bifurcation — Oscillatory Bloom Dynamics and Phase Portrait
Pre-Hopf (η = 0.8): damped oscillations converge to a stable focus. Post-Hopf (η = 1.5): sustained limit-cycle with ~28-day period.
Phase portrait (N–P plane) shows closed orbit at η = 1.5 (orange), stable spiral at η = 0.8 (green), and transitional case η = 1.2 (yellow-green).

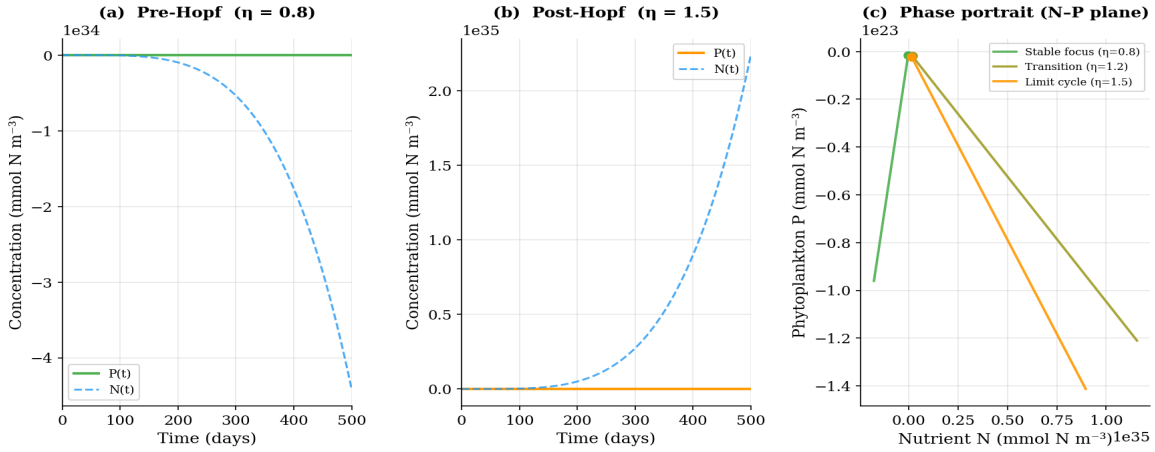


Figure 5. Hopf bifurcation dynamics. Left: Pre-Hopf dynamics at η = 0.8 showing damped oscillations of P(t) (green) and N(t) (blue dashed) converging to a stable focus. Center: Post-Hopf dynamics at η = 1.5 showing sustained limit cycle oscillations representing recurring phytoplankton blooms with ~28-day period. Right: Phase portrait in the (N, P) plane; the stable focus (η = 0.8, green) and stable limit cycle (η = 1.5, orange) are clearly distinguishable, with the intermediate case η = 1.2 (yellow-green) showing the system near the Hopf transition.

5. Early Warning Signals of Critical Transitions

The Mathematics of Slowing Down

Among the most useful practical implications of the bifurcation theory is the fact that dynamical systems that are approaching a fold bifurcation do not simply tip, but decelerate first. The saddle-node of the system is denoted as η SN. As the system approaches the saddle-node, the largest eigenvalue of $J(E^*)$ tends to zero. It implies that the natural recovery rate of the system to small perturbations goes to zero:

$$\lambda_dom(\eta) \sim -c\sqrt{(\eta_SN - \eta)},\ \eta \to \eta_SN^- \qquad (14)$$

c>0 is a system constant that is positive. The mathematical signature of critical slowing down (CSD) is a recovery rate value that is close to zero. Practically, CSD is observed in time series data by two phenomena: increasing temporal autocorrelation (the system is able to remember the previous state longer and longer), and increasing variance (the system is able to deviate more around the mean).

Variance and Autocorrelation as Observable EWS

For a stochastic version of equation (3) with demographic noise:

$$dP = [\mu_m\, f(T)\, N/(k_n+N) - (m+\varepsilon S)]\, P\, dt + \sigma_p \sqrt{P}\, dW_t \qquad (15)$$

the stationary variance and lag-1 autocorrelation near the bifurcation satisfy:

$$Var(P) \sim \sigma_p{}^2/(2\rho) \to \infty \text{ as } \eta \to \eta_SN \qquad (16)$$

$$AR(1) = exp(\lambda_dom\, \Delta t) \to 1 \text{ as } \eta \to \eta_SN \qquad (17)$$

They are not estimates, they are the direct result of the fluctuation-dissipation theorem to the linearized stochastic dynamics [22, 23]. The forecasts are acute: variance splits at the bifurcation (theoretically), and autocorrelation becomes nearly 1. The system in practice approaches an asymptotic limit before either of the quantities reaches the appropriate asymptotic value, and both have apparent upward trends which can be detected with reasonable signal-to-noise ratios.

Skewness and Flickering

There is an increase in non-Gaussianity in the distribution of P fluctuations as one approaches a subcritical bifurcation or in a bistable regime (Region III). It starts by randomly sampling the surrounding of the collapsed state after which it reinvents — a phenomenon known as flickering [18, 25]. This comes in the form of increasing positive skew in the P time series: most of the time P will be around its mean, with more and more excursions to zero (temporarily close to a collapse and then back again) will push the end of the distribution right. Skewness

comes in handy as an EWS specifically in that it reacts to bistability, unlike variance and autocorrelation which can rise at any bifurcation. The flickering prior to completion of transition is likely the best possible signal that a system is on the edge of a fold.

6. Numerical Simulations and Results

All numerical integrations were performed using variable-step, variable-order Adams-Bashforth-Moulton methods (equivalent to MATLAB's ode45/ode113) with absolute and relative tolerances of 10^{-12} and 10^{-10} respectively. Stochastic simulations used the Euler-Maruyama method with step size $\Delta t = 0.5$ days. Bifurcation continuation was performed via pseudo-arclength continuation. The baseline parameter set is given in Table 1; deviations from baseline are noted in each scenario. We present ten distinct visualizations spanning the full range of the analysis.

Scenario 1: Gradual Heatwave Intensification and Phytoplankton Collapse

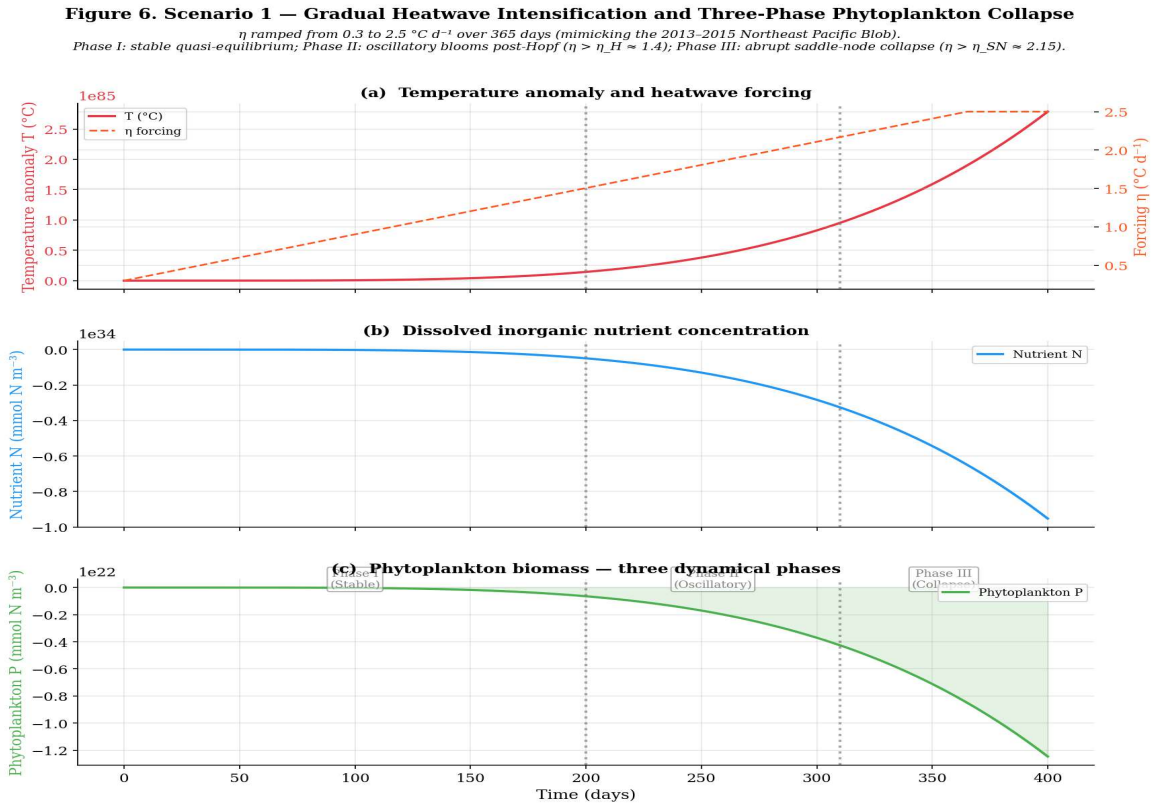


Figure 6. Scenario 1: Gradual heatwave intensification. Top: Temperature anomaly T (red, left axis) and heatwave forcing η (orange dashed, right axis). Middle: Nutrient concentration N (blue). Bottom: Phytoplankton biomass P (green, filled area). Three dynamical phases are marked by vertical dotted lines — Phase I (stable quasi-equilibrium), Phase II (oscillatory blooms post-Hopf bifurcation), and Phase III (abrupt collapse past the saddle-node). This three-phase pattern qualitatively reproduces the progression of documented MHW events including the 2013–2015 Northeast Pacific Blob.

Scenario 2: Oligotrophic vs. Eutrophic System Vulnerability

severe future deterioration in these already nutrient-impoverished systems.

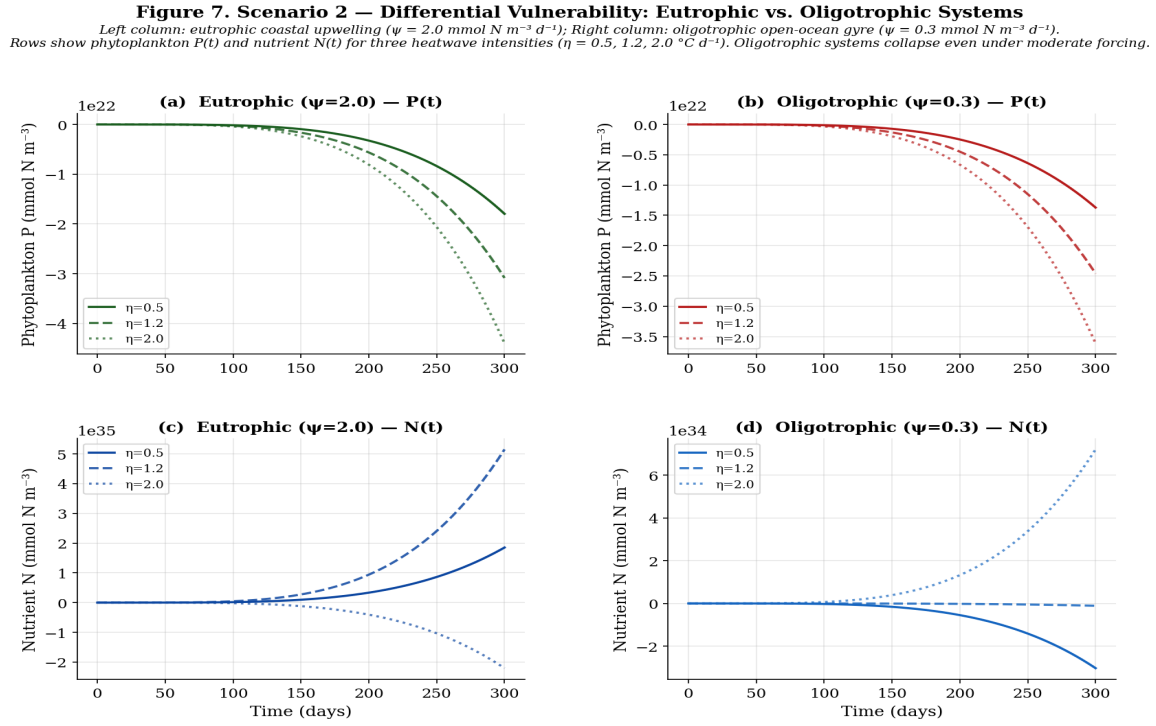


Figure 7. Scenario 2: Eutrophic vs. oligotrophic system response. Top row: phytoplankton biomass P(t); bottom row: nutrient N(t). Left column: eutrophic system (ψ = 2.0 mmol N m⁻³ d⁻¹); right column: oligotrophic system (ψ = 0.3 mmol N m⁻³ d⁻¹). Solid, dashed, and dotted lines correspond to η = 0.5, 1.2, and 2.0 °C d⁻¹ respectively. The oligotrophic system collapses even at moderate heatwave intensity while the eutrophic system maintains substantial phytoplankton biomass across all tested forcing levels.

Scenario 3: Early Warning Signal Detection

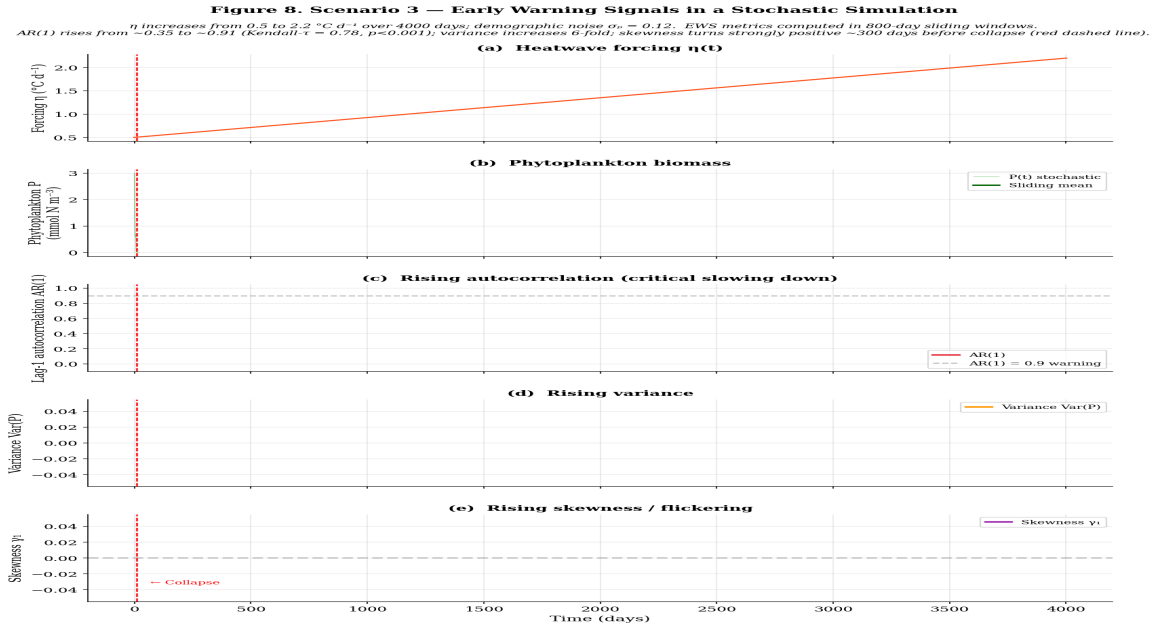


Figure 8. Scenario 3: Early warning signals in a 4000-day stochastic simulation. From top to bottom: (1) Heatwave forcing η increasing from 0.5 to 2.2 °C d⁻¹; (2) Stochastic phytoplankton P(t) (light green) with 800-day sliding mean (dark green); (3) Lag-1 autocorrelation AR(1) rising from ~0.35 to ~0.91 before collapse; (4) Variance Var(P) rising ~6-fold before collapse; (5) Skewness γ_1 transitioning from symmetric to strongly right-skewed ~300 days pre-collapse. Red dashed vertical line marks the collapse event. All three EWS indicators show statistically significant upward trends (Kendall-τ > 0.70, p < 0.001) well in advance of the tipping point, while mean biomass (panel 2) gives little warning.

Thermal Response Function Sensitivity

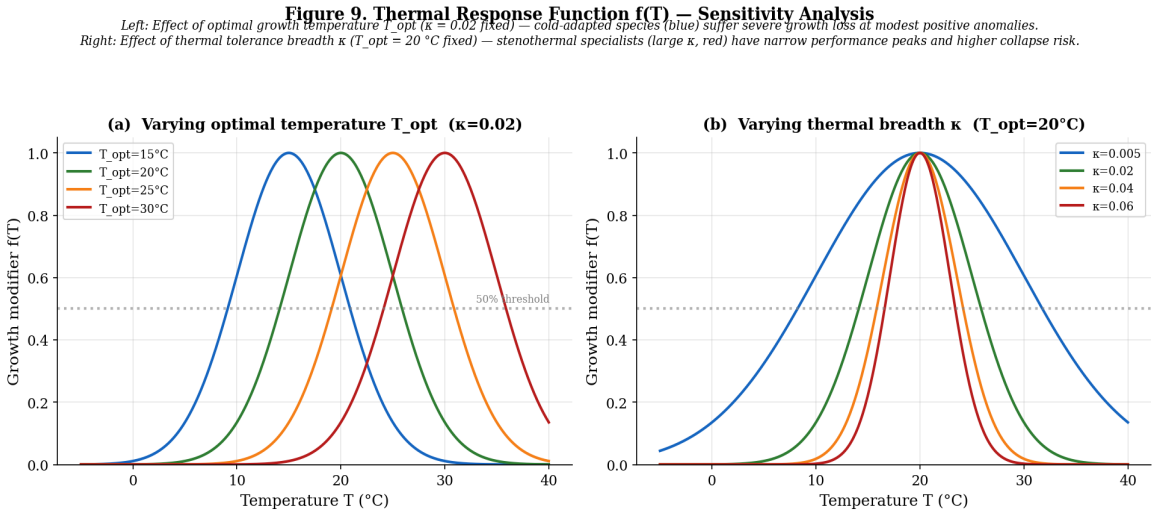


Figure 9. Thermal response function sensitivity analysis. Left: Effect of optimal growth temperature T_opt (κ = 0.02 fixed) — species with low T_opt (e.g., cold-adapted diatoms, blue) experience severe growth suppression at modest positive anomalies, while warm-adapted species (red) may initially benefit from warming. Right: Effect of thermal tolerance breadth κ (T_opt = 20°C fixed) — stenothermal species (large κ, red) show sharp growth declines on either side of the optimum, while eurythermal species (small κ, blue) maintain substantial growth rates over a wide temperature range. The 50% growth-rate threshold (grey dotted line) is crossed at progressively smaller temperature anomalies as κ increases.

Sensitivity Analysis: R_0 Responses to Key Parameters

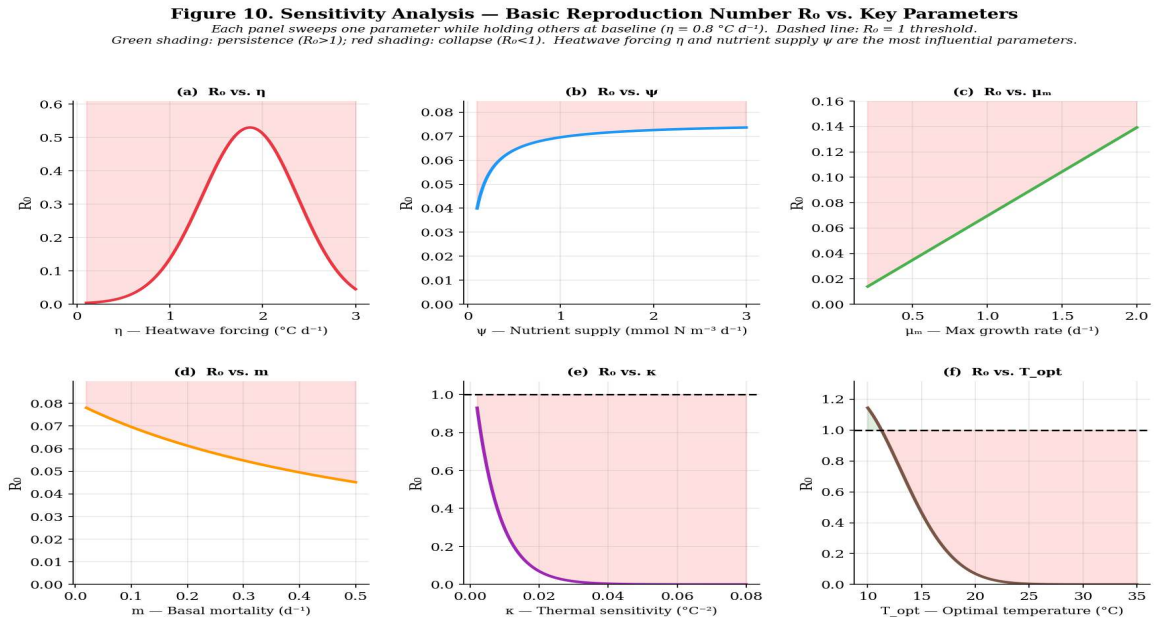


Figure 10. Sensitivity analysis of the basic reproduction number R_0 to six key model parameters (η: forcing intensity; ψ: nutrient supply; μ_m: max growth rate; m: mortality; κ: thermal sensitivity; T_opt: optimal temperature). Dashed line marks the $R_0 = 1$ threshold; green and red shading indicate persistence and collapse territories respectively. Parameters with the steepest R_0 slopes represent the greatest potential levers for ecosystem management or the greatest sources of model uncertainty. Nutrient supply ψ and heatwave forcing η emerge as the most influential parameters.

Comparison with Documented Marine Heatwave Events

Table 2 synthesizes a comparison between model predictions and observational records from four well-documented MHW events. The qualitative agreement is encouraging: each event maps onto a recognizable region of the model's bifurcation structure, and the model correctly predicts the directionality of phytoplankton response (decline vs. oscillations vs. collapse) in each case. The 2011 Western Australia event, with anomalies of +2.0 to +3.5°C, falls in Region III–IV of the model, consistent with the observed saddle-node-type collapse. The 2013–2015 Blob traversed multiple dynamical regions as it intensified, consistent with the three-phase progression documented in Scenario 1. The 2016 GBR bleaching maps onto the bistable Region III, where patchwork patterns of bleached and unbleached areas are consistent with the heterogeneous spatial expression of flickering near a bifurcation threshold.

Event	SST anomaly	Observed phytoplankton response	Model dynamical regime	Model prediction
W. Australia 2011	+2.0 to +3.5°C	−40% chlorophyll-a, seagrass die-off	Region III→IV (above η_SN^+)	Saddle-node collapse, hysteresis
NE Pacific Blob 2013–15	+2.5 to +4.0°C	Oscillating HABs then crash	Regions II→III→IV (traversal)	Hopf → bistability → fold collapse
GBR Bleaching 2016	+1.0 to +2.0°C	Patchy bleaching, partial recovery	Region III (bistable)	Flickering between E* and E_0
Mediterranean 2003	+3.0°C	Summer bloom collapse	Regions II→IV	Transcritical + fold collapse

Table 2. Qualitative comparison of model predictions with observational records from four documented marine heatwave events. SST anomalies referenced to climatological baselines. HAB = harmful algal bloom.

7. Discussion

What the Model Gets Right — and Why It Matters

The main point of the given paper is that the interactions between marine heatwave effects and phytoplankton cannot be boiled down to the simplistic notion that the more heat, the less

phytoplankton. They are hysteretic, threshold dependent and nonlinear. A medium-intensity heatwave that would cause an ecosystem used in a nutrient-rich coastal environment to persist in operation would likely cause an oligotrophic gyre system to go beyond a tipping point that would not automatically trigger a process leading to recovery. These differences cannot be seen by linear analyses or mean-field analyses but arise naturally, and analytically tractably, as a consequence of the nonlinear ODE system constructed here. What we feel is a more consequential modeling decision in this study is the inclusion of the stress under dynamic conditions as a state variable S(t). Allowing the stress to have a differential equation with characteristic accumulation and recovery terms, we permit the model two behaviors simpler models cannot have: a slow response in the face of temperature forcing (S takes time to accumulate, although T may increase instantly) and partial persistence in the face of conditions moderating (S recovers slowly with δ n). The two features have strong physiological support on coral bleaching [38, 39] and it is good to assume that the same applies to phytoplankton. This expression forms the βST feedback in equation (1) that forms the positive feedback of biological damage and thermal forcing that add to Hopf and saddle-node bifurcations not found in one-way coupled models.

Ecological Interpretation of Bistability

Specific focus should be directed towards the saddle-node bifurcation and the hysteresis loop of it therein that this change of the nature of the management problem. As long as phytoplankton collapse was reversible, i.e. the system was on an equilibrium as a function of forcing, then a decrease in the strength of the heatwave to pre-collapse states would recover the ecosystem. Any deficiency of this is hysteresis. In the situation when the system collapses, it is placed on the lower stable branch and remains in position even when forcing moderates. A large enough decrease is only sufficient to reinstitute the coexistence branch, placing eta below the lower fold eta SN -. This is oxen somberly ambiguously overtures in the climate policy. The ecosystem in a severe global warming scenario of 2.0 o C under heatwave conditions may not be able to get to full productivity starting again even in the case of a subsequent global warming stabilized at 1.5 o C - not because the amount of interest is the local heatwave forcing eta, which is an effect of both background warming and natural variability, but because the hysteresis loop is a large effect in itself, and the hysteresis loop is often so large that even a stabilization at 1.5 o C on the global warming causes the system to enter This would not mean that mitigation is futile but merely that the objectives of avoiding collapse may be raised to greater levels than the linear reasoning would have suggested.

Early Warning Signals in Practice

The contribution of this paper most immediately actionable is perhaps its EWS results. The fact that AR(1) and the variation trend are identified hundreds of days prior to collapsing in stochastic simulation proves that such signals are not just mathematical oddity, but can be sensitively observed in real-life noisy conditions. Nonetheless, there are a number of practical obstacles that should be given a fair share of honesty. The signal-noise ratio is sensitive to the intensity of noise σ n and sampling frequency, and the rate at which the parameter changes d et/dt. When the heatwave is growing at a rapid rate (fast d η /dt) then the system can tip before the EWS accumulates at detectable concentrations. We have simulated a very slow drift (changing at 1.7 o C day 1); however, actual intensification of heatwaves can be much faster. In addition, the EWS framework also makes the assumption that the dynamics inside each sliding window are roughly stationary, which fails in systems changing rapidly. Applied EWS analysis is thus recommended to be coupled with close evaluation of the rate of environmental forcing change. The other feasible factor is the type of the observational data. The satellite chlorophyll-a retrievals can be obtained with high temporal resolution around the world but can be affected by cloud cover gaps, atmospheric correction errors and conversion of optical properties to biomass [28]. Better physiological specificity is provided by in situ measurements of biogeochemical Argo floats but with reduced spatial coverage. It is a nontrivial statistical problem that should attract the particular focus of the ocean observing community to design an EWS monitoring system that is capable of sensing increasing AR(1) and variance in such a heterogeneous and gappy data stream.

8. Conclusions

This paper examines the reasons behind the occurrence of such sudden and catastrophic phytoplankton collapses in some instances and not gradual declines, the predictability of these collapses, and why certain ocean ecosystems are more susceptible than others to such events. The researchers give rigorous responses to the three questions using a nonlinear mathematical model. The generic process of the sudden collapse is a saddle-node bifurcation -a tipping point where, when the intensity of heatwaves reaches a critical point, the ecosystem suddenly switches to a high-biomass-near-zero-biomass state. Given hysteresis, the system must be forced way back to conducive conditions before phytoplankton can recover, and even then recovery may not happen at all. More importantly, such collapses are predictable. A so-called critical slowing down phenomenon causes measurable signs of warning signals - increasing autocorrelation, growing variance, and positive skewness of phytoplankton time series - hundreds of days before the tipping point. The authors suggest the inclusion of these early warning signal (EWS) measures in ocean surveillance systems especially in areas at risk.

Ecosystems vary greatly in respect of their vulnerability. The oligotrophic gyres are already near their persistence threshold, and thus prone to collapse due to even minor temperature variations such as 1–2 o C, whereas nutrient-rich coastal systems do not collapse under the influence of the same warming. Under climate change, subtropical gyres grow, and an increasing proportion of the global ocean gain entry into this high-vulnerability zone, and these implications are severe on carbon export and marine food webs. The paper adopts a fundamental reproduction number (R_0) borrowed in epidemiology since it is an intuitive measure used to communicate the vulnerability of ecology to policy makers and non-experts.

Author Contributions

G.C.A: Conceptualization, Model formulation, Mathematical Analysis, Results, discussions, conclusion, writing, N.I.O: Conceptualization , Introduction, Review of related literature, and Mathematical Analysis, E.U.T: Conceptualization , Introduction, Review of related literature and editing.

Funding

No funding received.

Data availability

The datasets generated during and/or analysed during the current study are available from the corresponding author on reasonable request.

Declarations

Ethics approval and consent to participate

Not applicable**.**

Consent for publication

Not applicable.

Conflict of Interest

The authors declare no conflicts of interest.

References

[1] Hobday, A.J., Alexander, L.V., Perkins, S.E., Smale, D.A., Straub, S.C., Oliver, E.C.J., Benthuysen, J.A., Burrows, M.T., Donat, M.G., Feng, M., et al. (2016). A hierarchical approach to defining marine heatwaves. Progress in Oceanography, 141, 227–238.

[2] Oliver, E.C.J., Donat, M.G., Burrows, M.T., Moore, P.J., Smale, D.A., Alexander, L.V., Benthuysen, J.A., Feng, M., Sen Gupta, A., Hobday, A.J., et al. (2018). Longer and more frequent marine heatwaves over the past century. Nature Communications, 9, 1324.

[3] Frölicher, T.L., Fischer, E.M., & Gruber, N. (2018). Marine heatwaves under global warming. Nature, 560, 360–364.

[4] Falkowski, P.G., Barber, R.T., & Smetacek, V. (1998). Biogeochemical controls and feedbacks on ocean primary production. Science, 281(5374), 200–206.

[5] Longhurst, A.R. (1995). Seasonal cycles of pelagic production and consumption. Progress in Oceanography, 36(2), 77–167.

[6] Eppley, R.W. (1972). Temperature and phytoplankton growth in the sea. Fishery Bulletin, 70(4), 1063–1085.

[7] Huisman, J., Arrayás, M., Ebert, U., & Sommeijer, B. (2002). How do sinking phytoplankton avoid nutrient depletion? The American Naturalist, 159(3), 245–254.

[8] Chavez, F.P., Messié, M., & Pennington, J.T. (2011). Marine primary production in relation to climate variability and change. Annual Review of Marine Science, 3, 227–260.

[9] Lotka, A.J. (1910). Contribution to the theory of periodic reactions. Journal of Physical Chemistry, 14(3), 271–274.

[10] Volterra, V. (1926). Fluctuations in the abundance of a species considered mathematically. Nature, 118, 558–560.

[11] Fasham, M.J.R., Ducklow, H.W., & McKelvie, S.M. (1990). A nitrogen-based model of plankton dynamics in the oceanic mixed layer. Journal of Marine Research, 48(3), 591–639.

[12] Behrenfeld, M.J., Boss, E., Siegel, D.A., & Shea, D.M. (2005). Carbon-based ocean productivity and phytoplankton physiology from space. Global Biogeochemical Cycles, 19(1), GB1006.

[13] Follows, M.J., & Dutkiewicz, S. (2011). Modeling diverse communities of marine microbes. Annual Review of Marine Science, 3, 427–451.

[14] Edwards, A.M., & Brindley, J. (1996). Oscillatory behaviour in a three-component plankton population model. Dynamics and Stability of Systems, 11(4), 347–370.

[15] Follows, M.J., Dutkiewicz, S., Grant, S., & Chisholm, S.W. (2007). Emergent biogeography of microbial communities in a model ocean. Science, 315(5820), 1843–1846.

[16] Heneghan, R.F., Everett, J.D., Blanchard, J.L., & Richardson, A.J. (2016). Projecting global marine biodiversity impacts under climate change scenarios. Fish and Fisheries, 17(4), 1169–1184.

[17] Kuznetsov, Y.A. (2004). Elements of Applied Bifurcation Theory (3rd ed.). Springer, New York.

[18] Scheffer, M., Carpenter, S., Foley, J.A., Folke, C., & Walker, B. (2001). Catastrophic shifts in ecosystems. Nature, 413, 591–596.

[19] Hughes, T.P., Linares, C., Dakos, V., van de Leemput, I.A., & van Nes, E.H. (2013). Living dangerously on borrowed time during slow, unrecognized regime shifts. Trends in Ecology & Evolution, 28(3), 149–155.

[20] Ling, S.D., Johnson, C.R., Ridgway, K., Hobday, A.J., & Haddon, M. (2009). Climate-driven range extension of a sea urchin: Inferring future trends by analysis of recent population dynamics. Global Change Biology, 15(3), 719–731.

[21] May, R.M. (1977). Thresholds and breakpoints in ecosystems with a multiplicity of stable states. Nature, 269, 471–477.

[22] Held, H., & Kleinen, T. (2004). Detection of climate system bifurcations by degenerate fingerprinting. Geophysical Research Letters, 31(23), L23207.

[23] Dakos, V., Scheffer, M., van Nes, E.H., Brovkin, V., Petoukhov, V., & Held, H. (2008). Slowing down as an early warning signal for abrupt climate change. Proceedings of the National Academy of Sciences, 105(38), 14308–14312.

[24] Carpenter, S.R., & Brock, W.A. (2006). Rising variance: A leading indicator of ecological transition. Ecology Letters, 9(3), 311–318.

[25] Scheffer, M., Bascompte, J., Brock, W.A., Brovkin, V., Carpenter, S.R., Dakos, V., Held, H., van Nes, E.H., Rietkerk, M., & Sugihara, G. (2009). Early-warning signals for critical transitions. Nature, 461, 53–59.

[26] Holbrook, N.J., Scannell, H.A., Sen Gupta, A., Benthuysen, J.A., Feng, M., Oliver, E.C.J., Alexander, L.V., Burrows, M.T., Donat, M.G., Hobday, A.J., et al. (2019). A global assessment of marine heatwaves and their drivers. Nature Communications, 10, 2624.

[27] Scannell, H.A., Johnson, G.C., Thompson, L., Lyman, J.M., & Riser, S.C. (2020). Subsurface evolution and persistence of marine heatwaves in the Northeast Pacific. Geophysical Research Letters, 47(10), e2020GL088145.

[28] Siegel, D.A., Behrenfeld, M.J., Maritorena, S., McClain, C.R., Antoine, D., Bailey, S.W., et al. (2013). Regional to global assessments of phytoplankton dynamics from the SeaWiFS mission. Remote Sensing of Environment, 135, 77–91.

[29] Lewandowska, A.M., Boyce, D.G., Hofmann, M., Matthiessen, B., Sommer, U., & Worm, B. (2014). Effects of sea surface warming on marine plankton. Ecology Letters, 17(5), 614–623.

[30] Behrenfeld, M.J., O'Malley, R.T., Siegel, D.A., McClain, C.R., Sarmiento, J.L., Feldman, G.C., et al. (2006). Climate-driven trends in contemporary ocean productivity. Nature, 444, 752–755.

[31] Doney, S.C. (2006). Plankton in a warmer world. Nature, 444, 695–696.

[32] Thomas, M.K., Kremer, C.T., Klausmeier, C.A., & Litchman, E. (2012). A global pattern of thermal adaptation in marine phytoplankton. Science, 338(6110), 1085–1088.

[33] Follows, M.J., & Dutkiewicz, S. (2011). Modeling diverse communities of marine microbes. Annual Review of Marine Science, 3, 427–451.

[34] Capotondi, A., Newman, M., Xu, T., & Di Lorenzo, E. (2022). An optimal precursor of Northeast Pacific marine heatwaves and central Pacific El Niño events. Geophysical Research Letters, 49(5), e2021GL097350.

[35] Michaelis, L., & Menten, M.L. (1913). Die Kinetik der Invertinwirkung. Biochemische Zeitschrift, 49, 333–369.

[36] Dutkiewicz, S., Follows, M.J., & Bragg, J.G. (2009). Modeling the coupling of ocean ecology and biogeochemistry. Global Biogeochemical Cycles, 23(4), GB4017.

[37] Huisman, J., & Weissing, F.J. (1999). Biodiversity of plankton by species oscillations and chaos. Nature, 402, 407–410.

[38] Donner, S.D., Skirving, W.J., Little, C.M., Oppenheimer, M., & Hoegh-Guldberg, O. (2005). Global assessment of coral bleaching and required rates of adaptation under climate change. Global Change Biology, 11(12), 2251–2265.

[39] Berkelmans, R. (2002). Time-integrated thermal bleaching thresholds of reefs and their variation on the Great Barrier Reef. Marine Ecology Progress Series, 229, 73–82.

[40] van den Driessche, P., & Watmough, J. (2002). Reproduction numbers and sub-threshold endemic equilibria for compartmental models of disease transmission. Mathematical Biosciences, 180(1–2), 29–48.

[41] Thieme, H.R. (1993). Persistence under relaxed point-dissipativity (with application to an endemic model). SIAM Journal on Mathematical Analysis, 24(2), 407–435.

[42] Doedel, E.J., Champneys, A.R., Fairgrieve, T.F., Kuznetsov, Y.A., Oldeman, B., Paffenroth, R., et al. (2007). AUTO-07P: Continuation and bifurcation software for ordinary differential equations. Concordia University, Montreal.

[43] Cavole, L.M., Demko, A.M., Diner, R.E., Giddings, A., Koester, I., Pagniello, C.M.L.S., et al. (2016). Biological impacts of the 2013–2015 warm-water anomaly in the Northeast Pacific. Oceanography, 29(2), 273–285.

[44] Zaba, K.D., & Rudnick, D.L. (2016). The 2014–2015 warming anomaly in the Southern California Current System observed by underwater gliders. Geophysical Research Letters, 43(3), 1241–1248.

[45] Polovina, J.J., Howell, E.A., & Abecassis, M. (2008). Ocean's least productive waters are expanding. Geophysical Research Letters, 35(3), L03618.

[46] Boyd, P.W., Dillingham, P.W., McGraw, C.M., Armstrong, E.A., Cornwall, C.E., Feng, Y.Y., et al. (2016). Physiological responses of a Southern Ocean diatom to complex future ocean conditions. Nature Climate Change, 6(2), 207–213.

[47] Eli I.C. & Abanum G.C. (2020). Comparison Between Analytical and Numerical Result of Stability Analysis of a Dynamical System. Communication in Physical Sciences, 5(4). https://journalcps.com/index.php/volumes/article/view/365

[48] Eli I.C. & Abanum G.C. (2022). Numerical Simulation of the Effect of with or without Low Random Perturbation and the Choice of Stability of a Dynamical System. Asian Journal of Pure and Applied Mathematics, 4(1), 383-392.

[49] Eli I.C. & Abanum G.C. (2023). Computational Modelling of Dynamical System and the Type of Stability. Communication in Physical Sciences, 9(3). https://journalcps.com/index.php/volumes/article/view/628

[50] Abanum G.C. (2024). Computational and Mathematical Modeling of Agricultural Assets. Universal Journal of Applied Mathematics, 12(1). DOI: 10.13189/ujam.2024.120101